PHOTOSYNTHETICA
International Journal for Photosynthesis Research

DOI 10.32615/ps.2024.025 PHOTOSYNTHETICA 62 (3): 240-251, 2024

Relationship between photosynthetic performance and yield loss in winter oilseed rape (*Brassica napus* L.) under frost conditions

P. DĄBROWSKI[*,+], Ł. JEŁOWICKI[**], Z.M. JASZCZUK[***], S. MAIHOUB[#], J. WRÓBEL[##], and H.M. KALAJI[###,+]

Department of Environmental Management, Institute of Environmental Engineering, Warsaw University of Life Sciences – SGGW, Nowoursynowska St. 159, 02-787 Warsaw, Poland[*]
OPEGIEKA Sp. z o.o., Aleja Tysiąclecia 11, 82-300 Elbląg, Poland[**]
Faculty of Agriculture and Ecology, Warsaw University of Life Sciences – SGGW, Nowoursynowska St. 159, 02-787 Warsaw, Poland[***]
Faculty of Civil Engineering Warsaw University of Life Sciences SGGW, Nowoursynowska St. 159, 02-787 Warsaw, Poland[#]
Department of Bioengineering, West Pomeranian University of Technology in Szczecin, al. Piastów 17, 70-310 Szczecin, Poland[##]
Department of Plant Physiology, Institute of Biology, Warsaw University of Life Sciences – SGGW, Nowoursynowska St. 159, 02-787 Warsaw, Poland[###]

Abstract

Winter oilseed rape (*Brassica napus* L.), the principal oilseed crop in Europe, is notably vulnerable to spring frosts that can drastically reduce yields in ways that are challenging to predict with standard techniques. Our research focused on evaluating the efficacy of photosynthetic efficiency analysis in this crop and identifying specific chlorophyll fluorescence parameters severely impacted by frost, which could serve as noninvasive biomarkers for yield decline. The experiments were carried out in semi-controlled conditions with several treatments: a control, one day at –3°C, three days at –3°C, one day at –6°C, and three days at –6°C. We employed continuous-excitation and pulse-amplitude-modulation chlorophyll fluorescence measurements to assess plant sensitivity to frost. Also, plant gas exchange and chlorophyll content index measurements were performed. Certain parameters strongly correlated with final yield losses, thereby establishing a basis for developing new agricultural protocols to predict and mitigate frost damage in rapeseed crops accurately.

Keywords: abiotic stresses; bioindicator; chlorophyll *a* fluorescence; noninvasive biomarkers; plant gas exchange; plant traits.

Highlights

- Some ChFl parameters have a strong correlation with final yield loss
- These parameters were also correlated with plant gas-exchange parameters
- Chlorophyll fluorescence can be used as a biomarker for yield decline after frost stress

Received 27 March 2024
Accepted 25 June 2024
Published online 31 July 2024

[+]Corresponding authors
e-mail: piotr_dabrowski@sggw.edu.pl
hazem@kalaji.pl

Abbreviations: ABS – energy fluxes of absorption of light energy; AL – actinic light; BBCH – Biologische Bundesanstalt, Bundessortenamt und Chemische Industrie; CCI – chlorophyll content index; ChFl – chlorophyll *a* fluorescence; C_i – substomatal CO_2 concentration; ET – electron transport; ETR – electron flow rate through photosystems; F_m' – maximum chlorophyll *a* fluorescence in light-adapted leaves; F_s – steady-state fluorescence at any light level; g_s – stomatal conductance; HPSC lamp – high-pressure sodium lamp; NPQ – nonphotochemical quenching, PAM – pulse-amplitude-modulation chlorophyll fluorescence, PC – plastocyanin; P_N – CO_2 assimilation; PQ – plastoquinone; RC – reaction center; TR – trapping of excitation energy; Φ_{PSII} (yield or Genty parameter) – estimated effective quantum yield (efficiency) of PSII photochemistry at given PAR.

Acknowledgements: The article was developed as part of the project titled "InsFlo – Fluorescence of crops in estimating losses caused by weather factors", implemented by OPEGIEKA Sp. z o.o., co-financed by the European Union from the European Regional Development Fund under the Smart Growth Operational Programme 2014-2020, Priority Axis I "Support for R&D activity of enterprises"', Measure 1.1 "R&D projects of enterprises", Sub-measure 1.1.1 "Industrial research and development work implemented by enterprises".
Conflict of interest: The authors declare that they have no conflict of interest.

Introduction

Winter oilseed rape (*Brassica napus* L.), recognized as Europe's leading oilseed crop, is widely cultivated across the continent (Tuck *et al.* 2006). The primary cultivation areas are in Germany, Poland, Lithuania, Latvia, France, and Italy (van Duren *et al.* 2015), where it is predominantly used for biofuel production, edible oil extraction, and as a supplement in livestock feed. With the progression of climate change, it is anticipated that the production of winter oilseed rape will increasingly face various adverse weather events, affecting production levels based on the prevailing climatic conditions (Pullens *et al.* 2019, 2021).

The dominance of winter oilseed rape varieties in Europe, coupled with their extended crop cycle, renders them highly susceptible to a broad spectrum of climatic conditions, including spring frost. Such conditions frequently result in significant reductions in both yield and production quality (Wei *et al.* 2017). Ice crystal formation within the intercellular spaces occurs when temperatures fall below 0°C, leading to cell dehydration. This dehydration results from differences in water potential inside and outside the cell, causing damage to cell membrane structures and adversely affecting plant physiology (Wang *et al.* 2023).

Traditionally, the estimation of yield losses in winter rapeseed has relied on classical methods that assess physical plant damage based on the assessor's judgment, such as counting healthy plants, and damaged flowers and pods. These conventional techniques are not only time-consuming and labor-intensive but also prone to considerable inaccuracies that bring conflicts between the customers (insured farmers) and the insurance companies.

It is important to note that physiological changes, such as the photosynthetic performance of plants, precede morphological alterations resulting from frost exposure (Peng *et al.* 2020). Photosynthesis, a crucial physiological process, exhibits high sensitivity to environmental changes. Plants' gas-exchange measurements are pivotal for studying photosynthesis and transpiration in plants as they provide direct insights into the exchange of gases, such as carbon dioxide and oxygen, which are fundamental to these processes. By measuring the rate at which carbon dioxide is assimilated, researchers can assess the efficiency of the photosynthetic machinery under various environmental conditions. Additionally, these measurements help in understanding stomatal behavior, which regulates both photosynthesis and transpiration. This dual insight into photosynthetic performance and water regulation makes gas-exchange measurements a comprehensive tool for studying plant responses to different stressors (Dąbrowski *et al*. 2019).

Nowadays, analyzing chlorophyll fluorescence (ChFl) kinetics stands out as an effective approach for gauging the effects of various stresses on photosynthesis, offering a robust means to assess the photochemical efficiency of this process. Such analysis is instrumental in uncovering insights about the elements engaged in the photosynthetic electron transfer process, with a particular focus on PSII, which is notably the most vulnerable component of the photosynthetic apparatus to environmental stresses, playing a pivotal role in the photosynthetic system's response to such conditions (Baker and Rosenqvist 2004, Kalaji *et al.* 2017a).

The primary methodologies for ChFl measurement include continuous-excitation chlorophyll fluorescence and pulse-amplitude-modulated (PAM) fluorescence. The continuous-excitation technique necessitates a preparatory dark adaptation of the leaf for about 20 min before conducting the measurement. This approach utilizes an actinic light (AL) source coupled with a detector to capture and convey the ChFl signal. The JIP-test stands out among the analytical methods for interpreting the acquired data. It plays a crucial role in assessing the functionality of PSII and its responsiveness to environmental changes (Kalaji *et al*. 2014, Dąbrowski *et al.* 2015). Drawing on the energy flow theory within thylakoid membranes, the JIP-test aids in elucidating the relationship between the biophysical properties of photosynthesis and the diverse fluorescence parameters, thereby offering a comprehensive understanding of PSII dynamics under various environmental conditions (Strasser *et al.* 2004, Živčák *et al.* 2014).

The PAM fluorescence method employs a modulated light source to induce ChFl that is switched on and off at predetermined frequencies. This modulation allows for the exclusive measurement of the variable component of the induced fluorescence, facilitating an in-depth analysis of the dynamic shifts in ChFl. By focusing on these variations, the PAM technique yields profound insights into the plant's photosynthetic efficiency, especially under stress conditions. An advantage of this method is that measurements can be conducted under ambient light conditions, including natural sunlight, as it effectively isolates the fluorescence signal from the background light. This capability enhances the versatility of PAM fluorescence in assessing photosynthetic activity in real-world environmental settings (Kalaji *et al.* 2017b).

Despite numerous studies investigating the effects of various stresses on ChFl, the literature lacks detailed information on leveraging parameters measured concurrently through both continuous-excitation and PAM fluorescence techniques to estimate yield losses in winter rapeseed caused by frost.

The goal of this study was to identify chlorophyll fluorescence (ChFl) and plant gas-exchange parameters highly sensitive to frost stress, serving as potential bioindicators of yield losses due to frost, and to find out the relationship between yield losses in winter oilseed rape (*Brassica napus* L.) due to frost based on the assessment of plants' photosynthetic performance. This can provide insights into the resilience and adaptability of rapeseed in adverse conditions.

Materials and methods

Experimental design and plant growth conditions: The experiment was carried out at Warsaw University

of Life Sciences, and consists of 80 pots. Winter oilseed rape plants (5 pcs.) (variety LG Areti, Limagrain, France, https://ChlFl.limagrain-europe.com/en) were sown in each pot at the beginning of September 2022. Each pot contains 6 kg of a substrate composed of 60% peat, 30% composted bark, and 10% sand. After preparing the mixture, 11 kg m^{-3} of chalk was added (to reach pH 6), followed by *MIS4* fertilizer + microelements (120 g m^{-3}) (*Intermag*, Poland). On 2 October 2022, 0.5% calcium nitrate + *Folium* 0.6% + *L Amino H* 0.6% (*Intermag*, Poland) was sprayed. On 5 October 2022, 3% $MgSO_4$ + *Radiculum* 0.6% (*Intermag*, Poland) was sprayed.

At this stage, all pots were placed in the vegetative hall under natural conditions for plant growth. No stress factors were introduced during this period. The most important meteorological conditions during the experimental period are presented below.

On 29 January 2023, all pots were transported into the closed part of the greenhouse, which led to the end of the plants' winter dormancy. During this period, the average daytime temperature was approximately 18°C. The sunlight exposure was equivalent to outdoor conditions, but the plants received supplementary illumination from a high-pressure sodium lamps (HPS lamp) with a light intensity of about 200 µmol(photon) m^{-2} s^{-1}. The humidity was maintained at around 70%.

On 8 March 2023, the plants reached the development stage BBCH 54 (flower buds of the main clusters compact and 50% uncovered by leaves). The pots were randomly divided into five groups, with 16 pots in each group. Each group constituted a separate research variant: (*1*) control (ambient temperature); (*2*) one-day frost –3°C; (*3*) frost –3°C for 3 consecutive days; (*4*) one-day frost –6°C; (*5*) frost –6°C for 3 consecutive days.

For stress application, plants were transferred from the greenhouse to growth chambers (cold phytotron, maintaining the same temperature as the greenhouse conditions) for 24 or 72 h. The temperature was gradually lowered at night to simulate natural frost stress in the field. The applied low temperatures (–3°C or –6°C) were maintained for at least 3 h. Other environmental conditions, such as PAR and humidity, were kept similar to those of the control plants grown in the greenhouse. Stress application was repeated during the BBCH 65–67 growth phase (full flowering: 50% of the flowers on the main inflorescence are open, and older petals fall off). Plant gas exchange, chlorophyll content index, and ChFl measurements were performed one week after stress application (28 April 2023). Subsequently, the plants were grown under natural conditions in the open part of the greenhouse until the end of the vegetation period, under the same conditions as the untreated control plants. The harvest was gathered on 5 July 2023.

Yield estimation: Plants underwent a natural desiccation process. Subsequently, seeds were obtained separately from each pot and then weighed to calculate the actual yield [t ha^{-1}].

Plant gas-exchange measurements and chlorophyll content index (CCI) measurement: The photosynthetic rate, in terms of net CO_2 assimilation (P_N), stomatal conductance (g_s), and substomatal CO_2 concentration (C_i), was measured on the same leaves as ChFl and CCI using a portable gas analyzer, *Lcpro+* (*ADC BioScientific Ltd*., UK). This open gas-exchange system operated in differential mode with a 150 mol s^{-1} flow rate of ambient air and light about 900 µmol(photon) m^{-2} s^{-1}. The measurements were taken after the stabilization of conditions in the chamber. The cuvette conditions were as follows: relative humidity (RH) of approximately 70%, air temperature of around 22°C, and CO_2 concentration of about 430 ppm. The stabilization time before measurement was not less than 5 min. Once the system had stabilized, the measurement was performed directly.

Chlorophyll *a* fluorescence: One leaf was selected for the measurement of chlorophyll *a* fluorescence on each plant, which was assessed using two fluorimeters: *HandyPEA* (*Hansatech Instruments Ltd*., United Kingdom) and *FMS-2* (*Hansatech Instruments Ltd*., United Kingdom).

All chlorophyll fluorescence (ChFl) parameters measured by *HandyPEA* after the dark adaptation (JIP-test) have been presented in Appendix 1.

Measurements by both fluorimeters were conducted on previously marked leaves, expecting to enhance the correlation index between ChFl signals and the final yield. One plant from each pot was chosen randomly. The mid-section of the leaf was dark-adapted for at least 25 min before measurements using special leaf clips. Each leaf sample was illuminated with continuous saturating actinic light [3,500 µmol(photon) m^{-2} s^{-1}] for 1 second.

Month	Average month temp. [°C]	Min. month temp. [°C]	Max. month temp. [°C]	Precipitation [mm]	Sunshine [µmol(photon) $m^{-2}s^{-1}$]	Humidity [%]
September 2022	12.6	3.2	17.2	56.0	832	77
October 2022	11.6	0.2	16.2	31.4	686	85
November 2022	4.4	–6.5	6.6	22.1	249	91
December 2022	0.8	–13.3	2.6	61.6	152	91
January 2023	3.6	–1.5	18.7	62.3	149	89
February 2023	1.8	–7.7	10.0	41.2	310	80
March 2023	4.9	–5.4	19.4	26.7	576	74
April 2023	9.4	–3.4	22.9	57.2	913	70

The measurements of PAM fluorescence performed by the *FMS-2* fluorimeter were conducted in a very close spot immediately after continuous-excitation ChFl measurements. During PAM measurements, a standard protocol of *Hansatech Instruments Ltd*. (UK) company (the producer of the *FMS-2* portable chlorophyll fluorescence measurements system) was used:

(*1*) By the use of special leaf clips, plants were adapted to darkness for about 15 min;

(*2*) First pulse of white light [4,000 µmol(photon) m^{-2} s^{-1}] was activated for 1 s (F_o and F_m measured);

(*3*) Waiting until the signal gets steady;

(*4*) Actinic white light [1,000 µmol(photon) m^{-2} s^{-1}] was activated (F_p measured);

(*5*) Waiting for 4–5 min until the signal gets a steady state (F_s was measured);

(*6*) A second pulse of white light [12,000 µmol(photon) m^{-2} s^{-1}] was activated for 1 s (F_m' measured).

These were measured six parameters:

F_s – steady-state fluorescence at any light level. This parameter indicates the intensity of chlorophyll fluorescence, which accompanies the photosynthesis process in stationary conditions;

F_m' – maximum chlorophyll *a* fluorescence in light-adapted leaves;

$\Phi_{PSII} = (F_m' - F_s)/F_m'$ – yield or Genty parameter – estimated effective quantum yield (efficiency) of PSII photochemistry at given PAR. Based on changes in the values of this parameter, the quantum yield of the photochemical reaction in PSII can be assessed;

$ETR = \Phi_{PSII} \times 0.84 \times 0.50 \times PAR$ – electron flow rate through photosystems;

$q_P = (F_m' - F_s)/(F_m' - F_o)$ – the photochemical quenching of variable chlorophyll fluorescence;

$q_N = (F_m - F_m')/(F_m - F_o)$ – the nonphotochemical quenching of variable chlorophyll fluorescence.

On this same leaf, the chlorophyll content index (CCI) measurements were made by using *CCM-200* (*Opti-Sciences*, *Inc.*, Hudson, USA) chlorophyll content meter.

Data analysis: In each treatment, 16 measurements of ChFl, CCI, and plant gas exchange (n = 16) were done. All the measured parameters were statistically analyzed by the *ANOVA* model and by *Fischer*'s test as a *post hoc* at a 0.05 confidence level using the *Statistica 10.0* program (*Statsoft*, *Inc*. Tulsa, USA). The mathematical relationship between chlorophyll fluorescence signals and yield losses was estimated by *Pearson*'s correlation coefficient at a 0.05 confidence level.

Results

Yield: The yield of winter oilseed rape was influenced by both the temperature and the duration of stress application (Fig. 1). Under control conditions, the yield was 3.84 t ha^{-1}. Exposure to frost at –3°C for 1 d significantly decreased yield by 7.7%. However, in plants subjected to this temperature for 3 d, the yield decreased by 35.2% compared to plants not exposed to stress. Frost at –6°C caused an even more significant decrease in yield, with reductions of 49.3% and 51.8% for 1-d and 3-d exposures, respectively.

Relative chlorophyll content and gas exchange: Under control conditions, the chlorophyll content index was 32.2 (a.u.). Exposure to frost did not cause a significant decrease in this parameter (Table 1). However, frost induced significant changes in all gas-exchange parameters. The CO_2 assimilation rate under control conditions was 22.3 µmol(CO_2) m^{-2} s^{-1}, and a significant decrease in this parameter was observed in plants subjected to all treatments except –3°C for 1 d. The lowest values were recorded under the –6°C treatment for 3 d. Stomatal conductance under control conditions was 0.34 mol(H_2O) m^{-2} s^{-1}, with a significant decrease confirmed in plants subjected to –6°C for both 1 and 3 d. Substomatal CO_2 concentration under control conditions was 238 µmol(CO_2) mol^{-1}, and a significant increase was noted in all treatments except –3°C for 1 d.

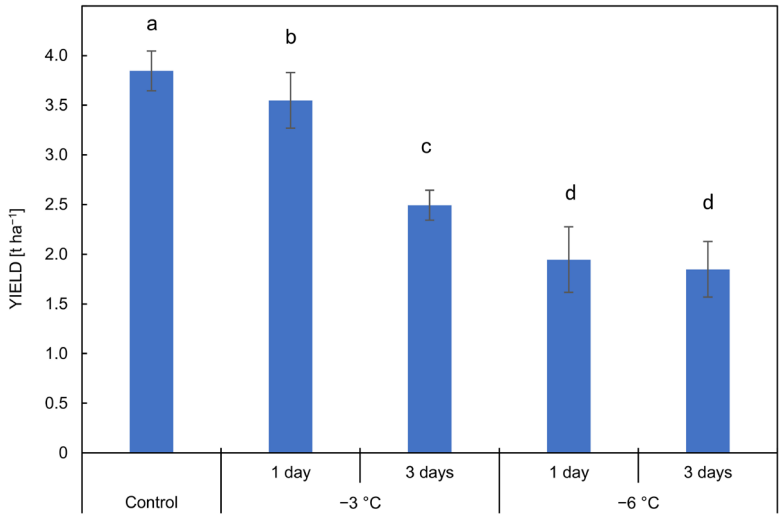

Fig. 1. The yield of winter oilseed rape decreased in the following order: control; one-day frost –3°C; frost –3°C for 3 consecutive days; one-day frost –6°C; frost –6°C for 3 consecutive days (t ha^{-1} ± SD). The means marked by the *same letter* indicate that the experimental variants did not differ significantly (p<0.05, n = 16).

Table 1. The dependence of gas-exchange parameters of the winter oilseed rape after the application of frost stress: control; one-day frost –3°C; frost –3°C for 3 consecutive days; one-day frost –6°C; frost –6°C for 3 consecutive days. CCI – chlorophyll content index; P_N – CO_2 assimilation; g_s – stomatal conductance, and C_i – substomatal CO_2 concentration. The means marked by the *same letter* indicate that the experimental variants did not differ significantly ($p<0.05$, $n = 16$).

Treatment	CCI [a.u.]		P_N [μmol(CO_2) $m^{-2}s^{-1}$]		g_s [mol(H_2O) $m^{-2}s^{-1}$]		C_i [μmol(CO_2) mol^{-1}]	
	mean	SD	mean	SD	mean	SD	mean	SD
Control	32.2^{a}	6.9	22.3^{a}	3.1	0.34^{a}	0.03	238^{b}	12
–3°C for 1 day	33.8^{a}	7.8	19.8^{ab}	2.9	0.29^{ab}	0.02	254^{ab}	15
–3°C for 3 days	31.2^{a}	12.1	18.9^{b}	2.2	0.28^{ab}	0.03	289^{a}	19
–6°C for 1 day	30.6^{a}	13.5	18.1^{bc}	2.4	0.24^{b}	0.02	293^{a}	11
–6°C for 3 days	29.4^{a}	14.5	16.2^{c}	1.5	0.22^{b}	0.01	308^{a}	14

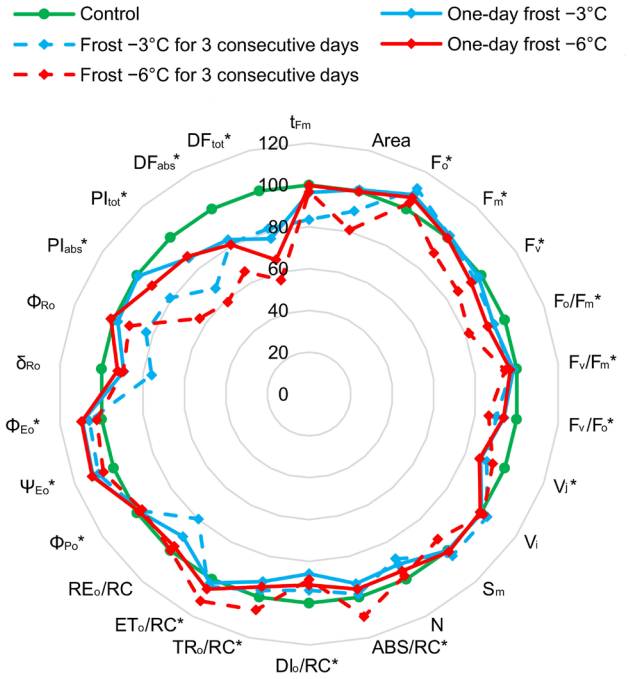

Fig. 2. The JIP-test parameters normalized to the values before stress application (control) as radar plots of winter oilseed rape in various frost treatments: control; one-day frost –3°C; frost –3°C for 3 consecutive days; one-day frost –6°C; frost –6°C for 3 consecutive days (a.u. ± SD). Means within particular parameters marked by the *asterisk* differ significantly from the control ($p<0.05$, $n = 16$).

JIP-test results: It was observed that certain parameters of the JIP-test exhibited heightened sensitivity to frost stress, as illustrated in Fig. 2. Among these parameters, those that showed a significant decrease in their values due to stress included: F_m, F_v, F_v/F_m, F_o/F_m, F_v/F_o, DI_o/RC, PI_{abs}, PI_{tot}, DF_{abs}, and DF_{tot}. On the other hand, some parameters exhibited a significant increase in their values, such as φ_{Eo} and ψ_{Eo}. The most substantial changes in the magnitude of these parameters were triggered by exposure to frost at –6°C for 3 d.

The shape of the OJIP induction curve was influenced by both the temperature and the duration of frost exposure, as depicted in Fig. 3. At the J point of the curve, a decrease was noted across all variations when compared to the control, with the most pronounced changes seen in plants subjected to frost for 3 d (Fig. 3*A*). At subsequent points of the curve (I and P), significant changes were observable exclusively in this specific variant. For the other variants, the curves followed a trajectory similar to that of the control.

After normalization and comparison of curves measured in control plants to stressed plants (where the curve always has a value of 0), differential curves were obtained (ΔV_t) (Fig. 3*B*). The purpose of this procedure is to highlight the differences between individual curves. Through this procedure, changes between individual variants can be visualized. Based on it, it was found that indeed the greatest changes occurred at point J.

PAM results: All parameters derived from PAM measurements were significantly affected by both the temperature and the duration of stress, as illustrated in Fig. 4. Under control conditions, the F_s parameter was 773 (a.u.). Exposure to frost at –3°C for 1 d significantly increased its value by 137%. In plants exposed to this temperature for 3 d, the value of this parameter increased by 149% compared to plants not subjected to stress. Frost at –6°C resulted in an even larger increase in this parameter, by 155% and 209% for 1-d and 3-d exposures, respectively. However, it should be noted that no significant differences were observed between the plants subjected to stress.

Under control conditions, the F_m' parameter was 3,208 (a.u.), and statistical analysis did not confirm the influence of frost at –3°C on this parameter. Exposure to frost at –6°C caused a reduction in this parameter to 74% and 70% of the control value for 1-d and 3-d exposures, respectively.

Under control conditions, the Φ_{PSII} parameter was 0.75 (a.u.), and statistical analysis confirmed the influence of frost at –3°C for 1 d on this parameter. Exposure to frost at –3°C for 3 d and at –6°C for both 1 and 3 d caused similar reductions in this parameter compared to the control.

It was observed that the ETR parameter also underwent reduction, with differences observed between the individual stress variants (both in terms of temperature and duration). Exposure to frost at –6°C for both 1 and 3 d caused a similar decrease in the photochemical quenching parameter (q_P) compared to the control. Conversely, nonphotochemical quenching (q_N) increased in all frost treatments, with an additional reduction observed at –3°C.

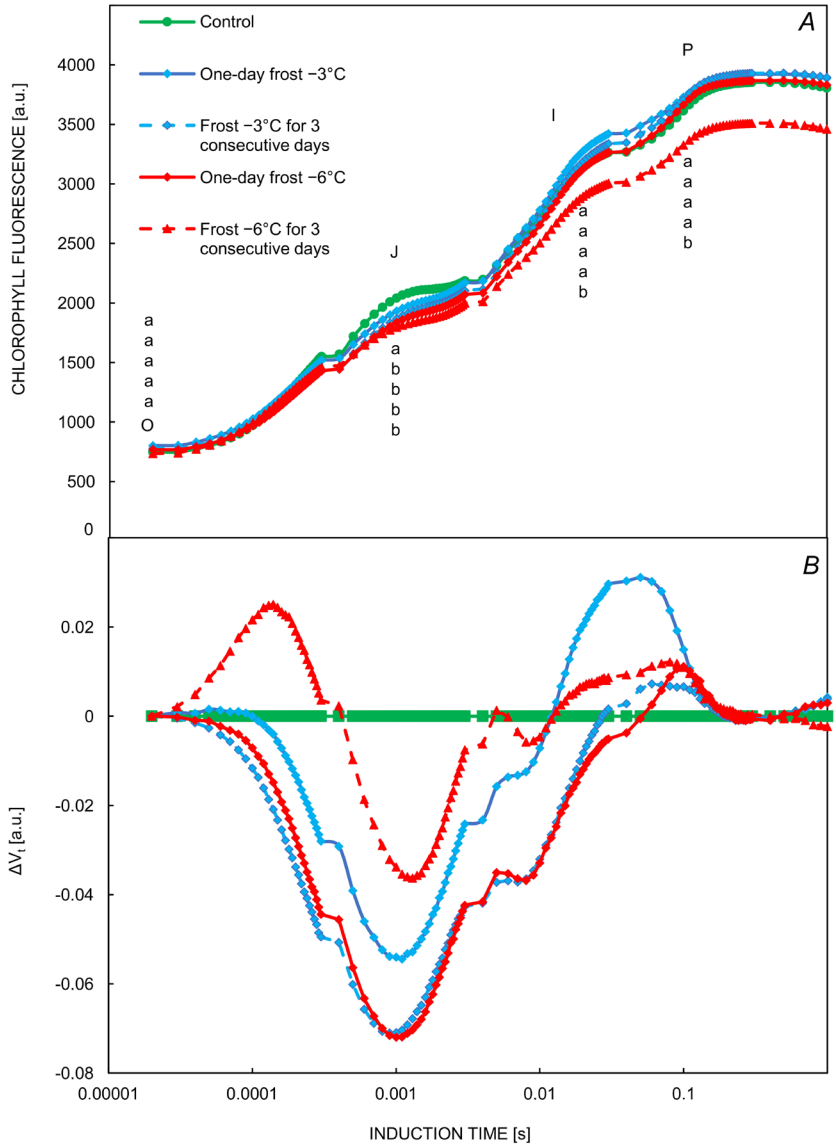

Fig. 3. Induction curves of chlorophyll *a* fluorescence (*A*) and differential curves of ΔV_t (obtained by subtracting the control curve from the first sample) (*B*) of winter oilseed rape in various frost treatments: control; one-day frost –3°C; frost –3°C for 3 consecutive days; one-day frost –6°C; frost –6°C for 3 consecutive days (a.u.) (n = 16, p<0.05).

Relationship between frost stress and individual photosynthetic activity parameters: Significant correlations were identified between all measured gas-exchange parameters and yield loss (Table 2). In the case of CO_2 assimilation (P_N) and stomatal conductance (g_s), this relationship was positive, meanwhile, in the case of intercellular CO_2 concentration (C_i), this relationship was negative. Some ChFl parameters were positively correlated: F_m', Φ_{PSII}, ETR, q_P, F_v/F_m, and J point from the OJIP curve. The values of the correlation coefficient of these parameters ranged from 0.89 to 0.95. Among the parameters negatively correlated was q_N (R = –0.96).

To evaluate how well the regression model fits the data, the coefficient of determination (R^2) was used, as it effectively indicates the proportion of variability in the dependent variable that the regression model can explain, as shown in Figs. 5, 6, and 7. The R^2 value for the equations that describe the relationship between crop yield loss and chlorophyll content index was 0.75. These values for gas-exchange parameters were even higher and fluctuated within the range from 0.84 to 0.96. The R^2 values for the equations that describe the relationship between crop yield loss and individual JIP-test parameters varied from 0.09 to 0.91. The highest value of R^2 was noted in J point. In comparison, the coefficient of determination values for the relationship between crop yield loss and PAM parameter values were higher, ranging from 0.67 to 0.92.

Discussion

The resilience of plants to frost stress encompasses a multifaceted trait, characterized by an array of physiological, biochemical, and molecular transformations (Fu *et al.* 2000, Kosová *et al.* 2012). In the quest for rapid and noninvasive evaluation of photosynthetic efficiency, several methodologies have been explored, among which spectral indices stand out. Predominantly utilized indices, ascertainable through compact, handheld devices, include the Photochemical Reflectance Index (PRI) and the

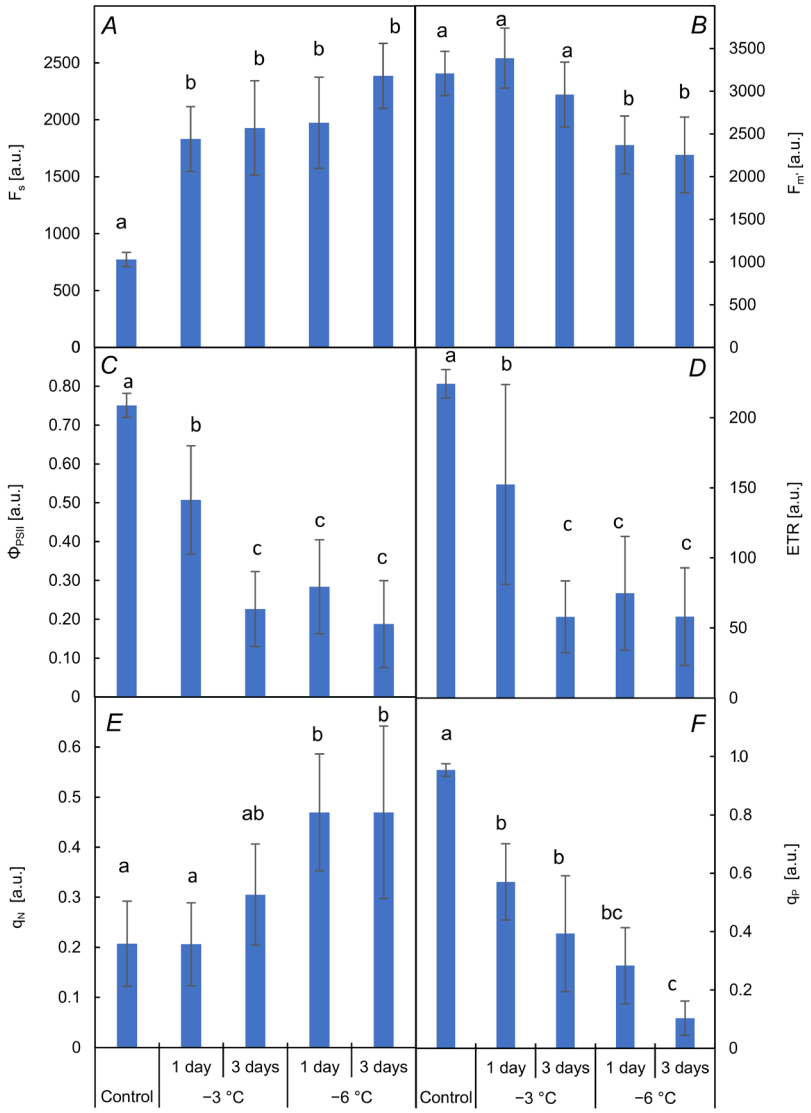

Fig. 4. The PAM (pulse-amplitude-modulation) parameters: steady-state fluorescence at any light level (F_s) (*A*), maximum fluorescence from light-adapted leaf (F_m') (*B*), estimated effective quantum yield (efficiency) of PSII photochemistry at given PAR (Φ_{PSII}) (*C*), electron transport rate (ETR) (*D*), nonphotochemical quenching (q_N) (*E*), and photochemical quenching (q_P) (*F*) of winter oilseed rape in various frost treatments: control; one-day frost –3°C; frost –3°C for 3 consecutive days; one-day frost –6°C; frost –6°C for 3 consecutive days. The means marked by the *same letter* do not differ significantly ($p<0.05$, $n = 16$).

Table 2. The *Pearson*'s correlation coefficient (*R*) between the yield of winter oilseed rape and individual parameters of photosynthetic activity under the influence of frost. All treatments were merged for this analysis. Values marked by an *asterisk* are significant ($n = 5$, $p<0.05$).

Parameter	*R*	Parameter	*R*	Parameter	*R*
CCI	0.86	F_v	0.84	ϕ_{Po}	0.78
P_N	0.91*	F_o/F_m	0.81	ψ_{Eo}	–0.40
g_s	0.93*	F_v/F_m	0.89*	ϕ_{Eo}	–0.23
C_i	–0.98*	PI_{inst}	0.14	δ_{Ro}	0.39
F_s	–0.82	F_v/F_o	0.78	ϕ_{Ro}	0.31
F_m'	0.93*	V_j	0.40	PI_{abs}	0.78
Φ_{PSII}	0.91*	V_i	–0.22	PI_{tot}	0.70
ETR	0.92*	S_m	0.34	DF_{abs}	0.82
q_P	0.93*	N	0.08	DF_{tot}	0.84
q_N	–0.96*	ABS/RC	–0.46	O	0.36
t_{Fm}	0.16	DI_o/RC	0.35	K	0.72
Area	0.63	TR_o/RC	–0.36	J	0.95*
F_o	–0.27	ET_o/RC	–0.85	I	0.64
F_m	0.56	RE_o/RC	–0.01	P	0.52

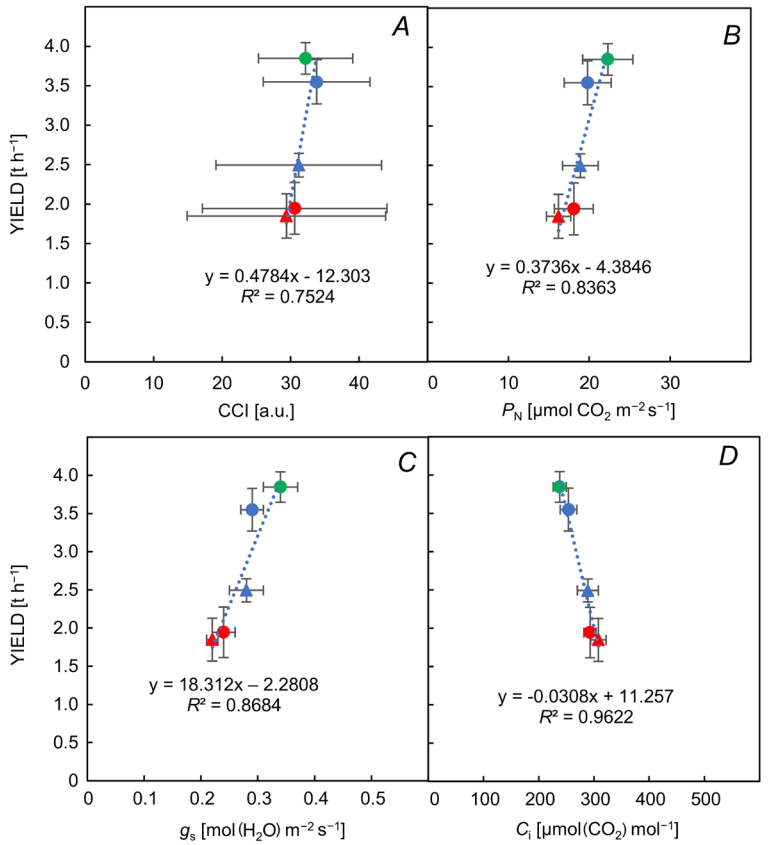

Fig. 5. The linear relationship between the yield of winter oilseed rape and chlorophyll content index and gas-exchange parameters: chlorophyll content index (CCI) (*A*), CO_2 assimilation (P_N) (*B*), stomatal conductance (g_s) (*C*), substomatal CO_2 concentration (C_i) (*D*). The point marked by a *green circle* is the control, by the *blue circle* is one-day frost –3°C, by the *blue triangle* is frost –3°C for 3 consecutive days, by the *red circle* is one-day frost –6°C and by the *red triangle* is frost –6°C for 3 consecutive days ($n = 16$, $p<0.05$).

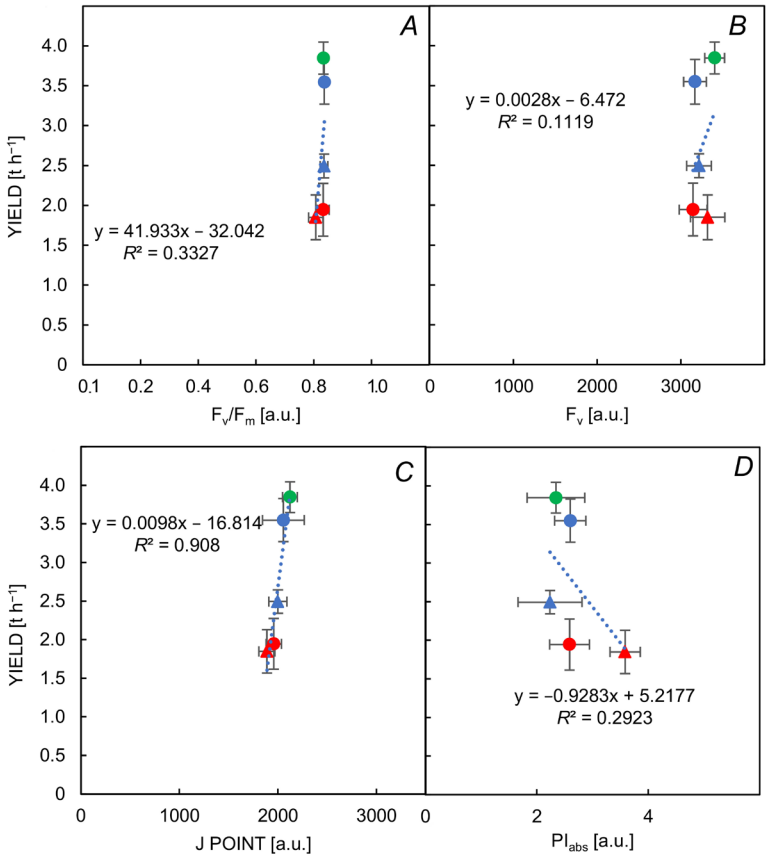

Fig. 6. The linear relationship between the yield of winter oilseed rape and chosen parameters of the JIP-test: maximum quantum yield for primary photochemistry (F_v/F_m) (*A*), variable fluorescence (F_v) (*B*), J point (*C*), and performance index per ABS (PI_{abs}) (*D*) under the influence of frost. The point marked by the *green circle* is the control, by the *blue circle* is one-day frost –3°C, by the *blue triangle* is frost –3°C for 3 consecutive days, by the *red circle* is one-day frost –6°C, and by the *red triangle* is frost –6°C for 3 consecutive days ($n = 16$, $p<0.05$).

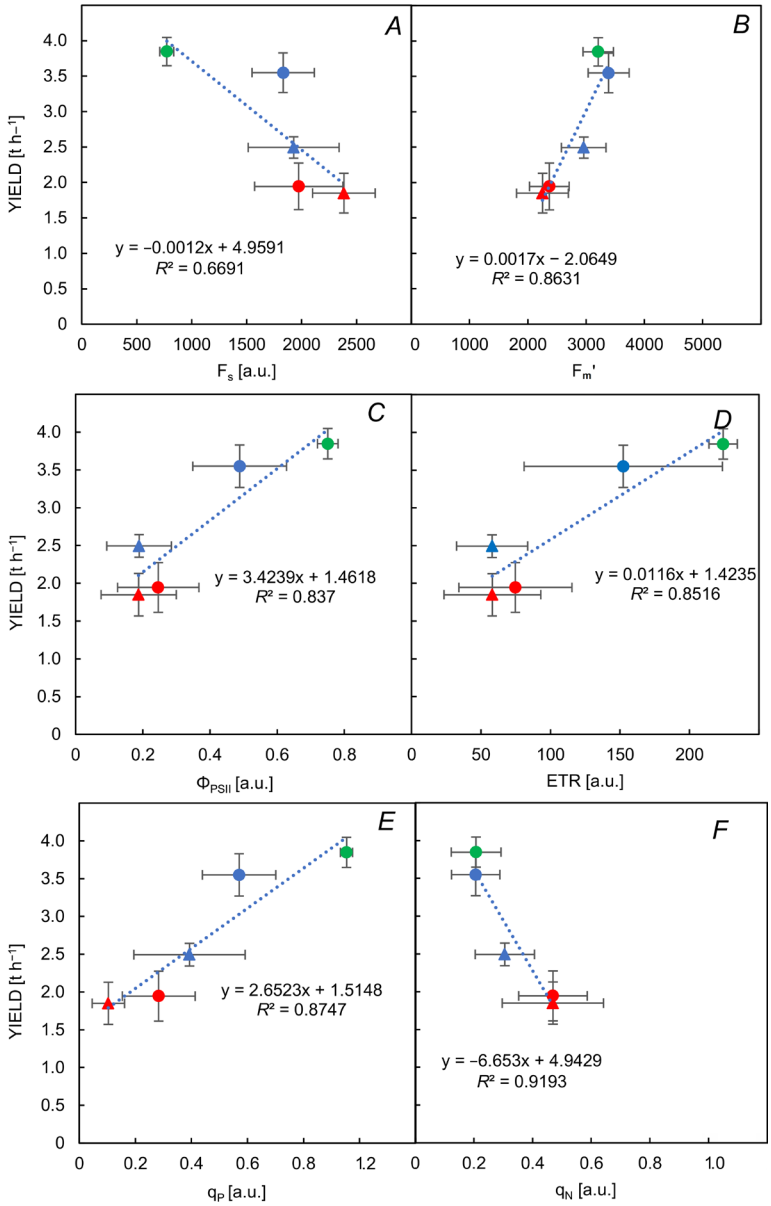

Fig. 7. The linear relationship between the yield of winter oilseed rape and chosen parameters of thePAM(pulse-amplitude-modulation):steady-state fluorescence at any light level (F_s) (*A*), maximum fluorescence from light-adapted leaf (F_m') (*B*), estimated effective quantum yield (efficiency) of PSII photochemistry at given PAR (Φ_{PSII}) (*C*), electron transport rate (ETR) (*D*), photochemical quenching (q_P) (*E*), and nonphotochemical quenching (q_N) (*F*) under the influence of frost. The point marked by the *green circle* is the control, by the *blue circle* is one-day frost –3°C, by the *blue triangle* is frost –3°C for 3 consecutive days, by the *red circle* is one-day frost –6°C, and by the *red triangle* is frost –6°C for 3 consecutive days ($n = 16$, $p<0.05$).

Normalized Difference Vegetation Index (NDVI) (Chytyk *et al.* 2011, Porcar-Castell *et al.* 2012). Nonetheless, these indices are not without their limitations, as their accuracy can be affected by variables other than photosynthetic efficiency, such as light intensity and air pollution. In contrast, chlorophyll fluorescence measurements, as suggested by studies (Chytyk *et al.* 2011, Urban *et al.* 2013), are perceived to be devoid of these constraints, offering a more reliable assessment of photosynthetic activity.

The core aim of our study was to investigate whether specific physiological parameters derived from gas-exchange measurements, continuous excitation, and PAM chlorophyll fluorescence parameters serve as reliable indicators of frost stress in winter oilseed rape under cold conditions. We posited that ChFl measurements could act as a dependable mechanism for tracking frost stress in oilseed rape before the manifestation of visible symptoms, attributing this capability to the association of this signal with photosynthetic efficiency.

Leaf photosynthesis is the most important source of energy for all autotrophic plants for growth and development. It is widely accepted that photosynthesis in C_3 plants under stress conditions is primarily limited by stomatal conductance and/or leaf biochemical capacity (Flexas and Carriquí 2020). Our studies confirmed that stomatal conductance, as well as CO_2 assimilation and H_2O transpiration, decreased in winter oilseed rape under frost stress. At the same time, intercellular CO_2 concentration increased. In the opinion of Dellero *et al.* (2021), those results may suggest that CO_2 accumulates within the intercellular spaces of the leaf when it is not assimilated by Rubisco. Moreover, these parameters significantly correlated with yield and also particular ChFl parameters,

so it is proved that they can be used as good indicators of plant stress (Dąbrowski *et al*. 2019).

A key finding from our research was the ability to identify points along the OJIP curve that exhibit sensitivity to frost stress. Our results indicated that the O point remained insensitive to frost stress, while the J point demonstrated the highest sensitivity, with its values fluctuating according to the stress intensity. The I and P points showed variations in their values solely under the most severe stress conditions. This pattern of sensitivity across the OJIP curve to frost stress in rapeseed plants corroborates findings from our earlier investigations and those conducted by Rapacz *et al.* (2015).

Additionally, when analyzing the specific JIP-test parameters, presented in a radar (or spider) plot format, it was evident that only some parameters were responsive to frost stress. This underscores the nuanced impact of cold temperatures on the physiological state of winter oilseed rape, highlighting the critical role of advanced fluorescence techniques in detecting and quantifying stress responses. This phenomenon can be well-followed based on the values of the F_v/F_m and specific energy fluxes. In all treatments, most of these measured and/or calculated parameters were significantly changed by this stress. These findings align with our earlier research (Stachurska *et al.* 2022). Furthermore, Rapacz *et al.* (2015), through field experiments, verified that the F_v/F_m parameter exhibits the strongest correlation with freezing tolerance. The observed reduction in the maximum photosynthetic efficiency of PSII in plants exposed to low temperatures may serve as a mechanism to protect PSII reaction centers, as noted by Rapacz and Hura (2002). Additionally, they reported a decrease in chlorophyll content in rape plants under frost stress, which could further contribute to the reduction in photosynthesis. Pons (2012) found that maintaining growth at low temperatures necessitates a significant investment in the photochemical apparatus to offset the diminished activity of enzymes.

Moreover, the sensitivity of performance index parameters (PI_{abs} and PI_{tot}) and driving forces (DF_{abs} and DF_{tot}) to frost stress was also confirmed by our studies. Frost stress elicited significant alterations in all four PAM parameters measured. These parameters are crucial for understanding the molecular dynamics of photosynthesis across various photosynthetic organisms under diverse biotic and abiotic stresses (Baker and Rosenqvist 2004, Mishra *et al*. 2016). According to numerous scholars, PAM analysis is deemed more complex than the OJIP analysis (Stirbet and Govindjee 2016, Bernát *et al.* 2018) because it encapsulates both photochemical and nonphotochemical quenching. This complexity arises from changes in thylakoid lumen acidification, ATP synthesis, and the activation of the Calvin–Benson cycle. F_s, or steady-state fluorescence in light-adapted plants illuminated with actinic light, reflects the relative fluorescence intensity. The quantum efficiency of PSII photochemistry diminishes as a result of the upregulation of nonphotochemical quenching mechanisms.

Upon illumination, PSII transitions from an “open” to a partly “closed” state, indicating that some PSII reaction centers are unable to utilize excitation energy effectively under light conditions. This increase in nonphotochemical de-excitation due to illumination is commonly denoted as NPQ (Kasajima *et al.* 2009). Our research confirmed that F_s is particularly sensitive to low temperatures, a phenomenon that can be attributed to the imbalance between the rates of ATP, NADPH synthesis, and CO_2 fixation. The Calvin–Benson cycle consumes less ATP and NADPH for CO_2 fixation than is generated by the primary processes of photochemical photosynthesis (Rapacz *et al*. 2004, Marečková *et al*. 2019). F_m' represents the maximum value of the fluorescence signal emitted by a sample exposed to stress and reflects changes in the rate constant of regulated nonphotochemical quenching. The changes in its values might express the extent of the regulated loss of nonphotochemical energy (Brestic *et al*. 2014). At the same time, a decrease in the Φ_{PSII} parameter at low temperatures can be attributed to cellular ice nucleation (Marečková *et al*. 2019).

The Φ_{PSII} parameter represents the fraction of the light energy absorbed by PSII that drives photosynthetic electron transport. It is frequently used in field research and might be interpreted as the effective quantum yield of the PSII photochemistry related to the actual fraction of photochemically active PSII reaction centers (q_P) (Roháček *et al.* 2008). It should be emphasized that our research confirms the high relationship between this parameter and yield losses (R = 0.91), with a coefficient of determination (R^2) of 0.837 for the linear relationship between these parameters. ETR represents one of the measures estimating the rate of photosynthetic processes in plant samples. ETR correlates well with the quantum yield of CO_2 assimilation and stomatal conductance (Perera-Castro and Flexas 2023, Sendall *et al*. 2024). Also, parameters indicating photochemical (q_P) and nonphotochemical quenching (q_N) had strong correlations with yield (0.93 and –0.96, respectively). Parameter q_P can be interpreted as the proportion of solar energy absorbed by PSII to the proportion of energy used by open reaction centers. Changes in this parameter provide information about the proportion of open reaction centers of PSII (Maxwell and Johnson 2000). At the same time, the increase in the q_N parameter under frost stress can be interpreted as an attempt to protect the photosynthetic apparatus by increasing the dissipation of absorbed energy in the form of heat (Demmig-Adams *et al*. 1996).

In conclusion, we recommend using plant photosynthetic efficiency measurements to monitor changes in winter oilseed rape, which can help estimate crop yield losses due to frost stress immediately after such events. Our findings enhance the understanding of crop susceptibility to sudden frost incidents. While this study did not directly compare the efficacy of different algorithms in forecasting crop yield losses, existing literature suggests that nonlinear algorithms like *Random Forests*, *Support Vector Machines*, and *Artificial Neural Networks* may outperform linear algorithms in processing chlorophyll fluorescence data for predicting yield losses (Peng *et al.* 2020). This research was conducted under partially controlled conditions and focused on a single crop variety. To build upon these

findings, future research should be carried out in field conditions and include a broader range of crop varieties to more thoroughly validate our conclusions.

References

Baker N.R., Rosenqvist E.: Applications of chlorophyll fluorescence can improve crop production strategies: an examination of future possibilities. – J. Exp. Bot. **55**: 1607-1621, 2004.

Bernát G., Steinbach G., Kaňa R. *et al.*: On the origin of the slow M–T chlorophyll *a* fluorescence decline in cyanobacteria: interplay of short-term light-responses. – Photosynth. Res. **136**: 183-198, 2018.

Brestic M., Zivcak M., Olsovska K. *et al.*: Reduced glutamine synthetase activity plays a role in control of photosynthetic responses to high light in barley leaves. – Plant Physiol. Biochem. **81**: 74-83, 2014.

Chytyk C.J., Hucl P.J., Gray G.R.: Leaf photosynthetic properties and biomass accumulation of selected western Canadian spring wheat cultivars. – Can. J. Plant Sci. **91**: 305-314, 2011.

Dąbrowski P., Baczewska-Dąbrowska A.H., Kalaji H.M. *et al.*: Exploration of chlorophyll *a* fluorescence and plant gas exchange parameters as indicators of drought tolerance in perennial ryegrass. – Sensors **19**: 2736, 2019.

Dąbrowski P., Pawluśkiewicz B., Baczewska A.H. *et al.*: Chlorophyll *a* fluorescence of perennial ryegrass (*Lolium perenne* L.) varieties under long term exposure to shade. – Žemdirbystė **102**: 305-312, 2015.

Dellero Y., Jossier M., Bouchereau A. *et al.*: Leaf phenological stages of winter oilseed rape (*Brassica napus* L.) have conserved photosynthetic efficiencies but contrasted intrinsic water use efficiencies at high light intensities. – Front. Plant Sci. **12**: 659439, 2021.

Demmig-Adams B., Adams III W.W., Baker D.H. *et al.*: Using chlorophyll fluorescence to assess the fraction of absorbed light allocated to thermal dissipation of excess excitation. – Physiol. Plantarum **98**: 253-264, 1996.

Flexas J., Carriquí M.: Photosynthesis and photosynthetic efficiencies along the terrestrial plant's phylogeny: lessons for improving crop photosynthesis. – Plant J. **101**: 964-978, 2020.

Fu P., Wilen R.C., Wu G.-H. *et al.*: Dehydrin gene expression and leaf water potential differs between spring and winter cereals during cold acclimation. – J. Plant Physiol. **156**: 394-400, 2000.

Kalaji H.M., Goltsev V.N., Żuk-Gołaszewska K. *et al.*: Chlorophyll Fluorescence: Understanding Crop Performance – Basics and Applications. Pp. 244. CRC Press, Boca Raton 2017b.

Kalaji H.M., Schansker G., Brestic M. *et al.*: Frequently asked questions about chlorophyll fluorescence, the sequel. – Photosynth. Res. **132**: 13-66, 2017a.

Kalaji H.M., Schansker G., Ladle R.J. *et al.*: Frequently asked questions about *in vivo* chlorophyll fluorescence: practical issues. – Photosynth. Res. **122**: 121-158, 2014.

Kasajima I., Takahara K., Kawai-Yamada M., Uchimiya H.: Estimation of the relative sizes of rate constants for chlorophyll de-excitation processes through comparison of inverse fluorescence intensities. – Plant Cell Physiol. **50**: 1600-1616, 2009.

Kosová K., Prášil I.T., Vítámvás P. *et al.*: Complex phytohormone responses during the cold acclimation of two wheat cultivars differing in cold tolerance, winter Samanta and spring Sandra. – J. Plant Physiol. **169**: 567-576, 2012.

Marečková M., Barták M., Hájek J.: Temperature effects on photosynthetic performance of Antarctic lichen *Dermatocarpon polyphyllizum*: a chlorophyll fluorescence study. – Polar Biol. **42**: 685-701, 2019.

Maxwell K., Johnson G.N.: Chlorophyll fluorescence – a practical guide. – J. Exp. Bot. **51**: 659-668, 2000.

Mishra K.B., Mishra A., Novotná K. *et al.*: Chlorophyll *a* fluorescence, under half of the adaptive growth-irradiance, for high-throughput sensing of leaf-water deficit in *Arabidopsis thaliana* accessions. – Plant Methods **12**: 46, 2016.

Peng B., Guan K., Zhou W. *et al.*: Assessing the benefit of satellite-based Solar-Induced Chlorophyll Fluorescence in crop yield prediction. – Int. J. Appl. Earth Observ. **90**: 102126, 2020.

Perera-Castro A.V., Flexas J.: The ratio of electron transport to assimilation (ETR/A_N): underutilized but essential for assessing both equipment's proper performance and plant status. – Planta **257**: 29, 2023.

Pons T.L.: Interaction of temperature and irradiance effects on photosynthetic acclimation in two accessions of *Arabidopsis thaliana*. – Photosynth. Res. **113**: 207-219, 2012.

Porcar-Castell A., Garcia-Plazaola J.I., Nichol C.J. *et al.*: Physiology of the seasonal relationship between the photochemical reflectance index and photosynthetic light use efficiency. – Oecologia **170**: 313-323, 2012.

Pullens J.W.M., Kersebaum K.C., Böttcher U. *et al.*: Model sensitivity of simulated yield of winter oilseed rape to climate change scenarios in Europe. – Eur. J. Agron. **129**: 126341, 2021.

Pullens J.W.M., Sharif B., Trnka M. *et al.*: Risk factors for European winter oilseed rape production under climate change. – Agr. Forest Meteorol. **272-273**: 30-39, 2019.

Rapacz M., Gasior D., Zwierzykowski Z. *et al.*: Changes in cold tolerance and the mechanisms of acclimation of photosystem II to cold hardening generated by another culture of *Festuca pratensis* × *Lolium multiflorum* cultivars. – New Phytol. **162**: 105-114, 2004.

Rapacz M., Hura K.: The pattern of changes in photosynthetic apparatus in response to cold acclimation and de-acclimation in two contrasting cultivars of oilseed rape. – Photosynthetica **40**: 63-69, 2002.

Rapacz M., Sasal M., Kalaji H.M., Kościelniak J.: Is the OJIP test a reliable indicator of winter hardiness and freezing tolerance of common wheat and triticale under variable winter environments? – PLoS ONE **10**: e0134820, 2015.

Roháček K., Soukupová J., Barták M.: Chlorophyll fluorescence: A wonderful tool to study plant physiology and plant stress. – In: Schoefs B. (ed.): Plant Cell Compartments – Selected Topics. Pp. 41-104. Research Signpost, Kerala 2008.

Sendall K.M., Muñoz C.M.M., Ritter A.D. *et al.*: Effects of warming and elevated CO_2 on stomatal conductance and chlorophyll fluorescence of C_3 and C_4 coastal wetland species. – Wetlands **44**: 43, 2024.

Stachurska J., Rys M., Pociecha E. *et al.*: Deacclimation-induced changes of photosynthetic efficiency, brassinosteroid homeostasis and *BRI1* expression in winter oilseed rape (*Brassica napus* L.) – relation to frost tolerance. – Int. J. Mol. Sci. **23**: 5224, 2022.

Stirbet A., Govindjee: The slow phase of chlorophyll *a* fluorescence induction in silico: Origin of the S–M fluorescence rise. – Photosynth. Res. **130**: 193-213, 2016.

Strasser R.J., Tsimilli-Michael M., Srivastava A.: Analysis of the chlorophyll *a* fluorescence transient. – In: Papageorgiou G.C., Govindjee (ed.): Chlorophyll *a* Fluorescence: A Signature of Photosynthesis. Advances in Photosynthesis and Respiration. Pp. 321-362. Springer, Dordrecht 2004.

Tsimilli-Michael M.: Revisiting JIP-test: An educative review on concepts, assumptions, approximations, definitions and

terminology. – Photosynthetica **58**: 275-292, 2020.
Tuck G., Glendining M.J., Smith P. *et al.*: The potential distribution of bioenergy crops in Europe under present and future climate. – Biomass Bioenerg. **30**: 183-197, 2006.
Urban M.O., Klíma M., Vítámvás P. *et al.*: Significant relationships among frost tolerance and net photosynthetic rate, water use efficiency and dehydrin accumulation in cold-treated winter oilseed rapes. – J. Plant Physiol. **170**: 1600-1608, 2013.
van Duren I., Voinov A., Arodudu O., Firrisa M.T.: Where to produce rapeseed biodiesel and why? Mapping European rapeseed energy efficiency. – Renew. Energ. **74**: 49-59, 2015.
Wang C., Wang Z., El-Badri A.M. *et. al.*: Moderately deep tillage enhances rapeseed yield by improving frost resistance of seedling during overwintering. – Field Crop. Res. **304**: 109173, 2023.
Wei C., Huang J., Wang X. *et al.*: Hyperspectral characterization of freezing injury and its biochemical impacts in oilseed rape leaves. – Remote Sens. Environ. **195**: 56-66, 2017.
Živčák M., Olšovská K., Slamka P. *et al.*: Measurements of chlorophyll fluorescence in different leaf positions may detect nitrogen deficiency in wheat. – Žemdirbystė **101**: 437-444, 2014.

Appendix 1. Glossary, definition of terms, and formulae used by the JIP-test for the analysis of the Chl *a* fluorescence transient OJIP emitted by dark-adapted photosynthetic samples (Tsimilli-Michael 2020, modified).

Parameter	Definition
t_{Fm}	time (in ms) to reach the maximal fluorescence F_P (meaningful only when $F_P = F_m$)
Area	total complementary area between the fluorescence induction curve and $F = F_P$ (meaningful only when $F_P = F_m$)
$F_o \cong$ F50µs or $\cong$ F20µs	fluorescence when all PSII RCs are open ($\cong$ to the minimal reliable recorded fluorescence)
F_m (= F_P)	maximal fluorescence, when all PSII RCs are closed (= F_P when the actinic light intensity is above 500 µmol(photon) m^{-2} s^1 and provided that all RCs are active as Q_A-reducing)
$F_v \equiv F_m - F_o$	maximal variable fluorescence
F_v/F_m	maximum quantum yield for primary photochemistry
$ABS/RC = M_o \times (1/V_J) \times (1/\phi_{Po})$	absorption flux (exciting PSII antenna Chl *a* molecules) per RC (also used as a unitless measure of PSII apparent antenna size)
$TR_o/RC = M_o \times (1/V_J)$	trapped energy flux (leading to Q_A reduction), per RC
$RE_o/RC = M_o \times (1/V_J) \times (1 - V_I)$	electron flux reducing end electron acceptors at the PSI acceptor side, per RC
$ET_o/RC = M_o \times (1/V_J) \times (1 - V_J)$	electron transport flux (further than Q_A^-), per RC
$DI_o/RC = (ABS/RC) - (TR_o/RC)$	energy flux not intercepted by an RC, dissipated in the form of heat, fluorescence, or transfer to other systems, at time t = 0
$\phi_{Po} \equiv TR_o/ABS = [1 - (F_o/F_m)]$	maximum quantum yield for primary photochemistry
$\phi_{Eo} \equiv ET_o/ABS = [1 - (F_o/F_m)] \times (1 - V_J)$	quantum yield for electron transport (ET)
$\phi_{Ro} \equiv RE_o/ABS = [1 - (F_o/F_m)] \times (1 - V_I)$	quantum yield for reduction of end electron acceptors at the PSI acceptor side (RE)
$\psi_{Eo} \equiv ET_o/TR_o = (1 - V_J)$	efficiency/probability that an electron moves further than Q_A^-
$\delta_{Ro} \equiv RE_o/ET_o = (1 - V_I)/(1 - V_J)$	efficiency/probability with which an electron from the intersystem electron carriers is transferred to reduce end electron acceptors at the PSI acceptor side (RE)
$N = S_m \times (M_o/V_J)$	turnover number (expresses how many times Q_A is reduced in the time interval from 0 to t_{Fm})
$S_m = (Area)/(F_m - F_o)$	normalized total area above the OJIP curve
PI_{abs}	performance index for energy conservation from photons absorbed by PSII until the reduction of intersystem electron acceptors
PI_{tot}	total performance index for energy conservation from photons absorbed by PSII until the reduction of PSI end electron acceptors
PI_{inst}	instrument-specific parameter
$DF_{abs} = \log(PI_{abs})$	PSII-relative driving force index on an absorption basis
$DF_{tot} = \log(PI_{tot})$	total PSII-relative driving force index